Polarization of ^{129}Xe with high power external-cavity laser diode arrays

J. N. Zerger,[a] M. J. Lim, K. P. Coulter, and T. E. Chupp
Department of Physics, University of Michigan, Ann Arbor, Michigan 48109-1120

(Received 7 December 1999; accepted for publication 3 February 2000)

We demonstrate narrowing of a 2 W, broad area laser diode array and present calculations of the resulting improvement of ^{129}Xe polarization by spin exchange with laser optically pumped Rb vapor. This improvement significantly impacts both medical imaging with laser polarized noble gas and spin-exchange pumped noble gas maser research. © *2000 American Institute of Physics*. [S0003-6951(00)02414-1]

High powered laser diode arrays (LDAs) and LDA bars are produced for a variety of commercial, industrial, and communications applications. One important application is optical pumping of alkali metals (e.g., Rb, K, Cs) to achieve nuclear polarization of ^{3}He, ^{129}Xe, and other noble gases via spin exchange. These polarized noble gases are used in a variety of applications, including fundamental physics measurements[1–3] and biomedical imaging research.[4–6]

A typical LDA spectrum (see Fig. 1) is comprised of many modes spread over wavelengths of 2 nm or more. In comparison, a homogeneously broadened Rb absorption line has widths of 0.1–0.2 nm. In spite of this apparent mismatch, LDAs can be very effective for optical pumping and polarization of noble gases, particularly ^{3}He.[7] Unfortunately, LDA optical pumping for polarization of ^{129}Xe is less effective. In this letter, we explain why this is the case, and we show that narrowing the spectral distribution should render LDAs much more effective for ^{129}Xe polarization. This has motivated the development of a simple, inexpensive, external–cavity configuration that we report here. We have narrowed a broad area commercial LDA to 20 GHz full width at half maximum (FWHM).

Optical pumping[8] manipulates the internal degrees of freedom of a sample of atoms through the transfer of angular momentum from photons to atoms.[9] For alkali-metal atoms, optical pumping can produce nearly complete polarization of the valence electron spin. This electron spin polarization is transferred to the nucleus of noble gas atoms by the hyperfine interaction during binary collisions[10] and, in the case of xenon, also during the lifetime of van der Waals molecules formed in three body collisions.[11–13]

Although the processes can be quite complex, the relevant physics is described by a single rate equation for the noble gas nuclear polarization.[14] In terms of the spin–exchange rate ($\gamma_{SE}=k_{SE}[A]$, where $[A]$ is the number density of the alkali-metal vapor and k_{SE} is the velocity averaged rate constant) and the relaxation rate Γ

$$\frac{d}{dt}P_I=\gamma_{SE}(P_A-P_I)-\Gamma P_I, \tag{1}$$

where $P_I=2\langle I_z\rangle$ is the rare gas nuclear polarization and $P_A=2\langle S_z\rangle$ is the volume averaged alkali-metal electron polarization. The steady state solution is

$$P_I=P_A\frac{\gamma_{SE}}{\gamma_{SE}+\Gamma}. \tag{2}$$

High polarization requires $\Gamma\ll\gamma_{SE}$ and P_A as large as possible.

Polarization of the alkali-metal valence electron by optical pumping can also be described by the rate equations for a two state system if the nuclear spin's effect of slowing the electron polarization rate is properly included.[15] The steady state, volume-averaged, alkali-metal electron spin polarization at any position is

$$P_A=2\langle S_z\rangle=\frac{\gamma_{opt}}{\gamma_{opt}+\Gamma_{SD}}, \tag{3}$$

where the position dependent optical pumping rate is

$$\gamma_{opt}(\mathbf{r})=\int d\nu\Phi(\mathbf{r},\nu)\sigma(\nu), \tag{4}$$

the cross section for absorption of unpolarized photons is $\sigma(\nu)$, and the laser intensity per unit frequency is $\Phi(\mathbf{r},\nu)=dI(\mathbf{r})/d\nu$. Destruction of electron spin polarization is accounted for by the rate Γ_{SD}. Rb spin relaxation is dominated by collisions with Rb atoms, rare gas atoms, N_2 molecules, and to a lesser degree, by wall interactions, which cause a layer of unpolarized Rb to form.[15] For Rb–^{3}He, the bulk spin destruction rate with no impurities is[15–17]

$$\Gamma_{SD}=k_{Rb-^3He}[^3He]+k_{Rb-N_2}[N_2]+k_{Rb-Rb}[Rb], \tag{5}$$

where the k's are rate constants for spin destruction due to collisions with each of the species in the target. For a typical ^{3}He application, $\Gamma_{SD}\approx 500$ Hz. For ^{129}Xe, Γ_{SD} is more complicated (due to three body interactions that lead to van der Waals molecule formation) and is on the order of tens of kHz. If γ_{opt} is not much larger than Γ_{SD}, the Rb polarization is significantly less than 100%, leading to strong attenuation of the incident circularly polarized laser photons and a lower average Rb polarization.

For ^{3}He, a large portion of the initial laser spectral profile is useful. In Fig. 1(a), we show the spectral profile at three positions along the axis of the cell for ^{3}He density of 10 amagat with 0.1 amagat N_2. As light burns its way into the cell, the central portion of the spectral profile is absorbed more strongly than the wings. Therefore, the front of the cell is essentially polarized by the near–resonance light, while the more off–resonance light is more important in the back of the cell. The large optical thickness of Rb typically used

[a]Author to whom correspondence should be addressed; electronic mail: jzerger@umich.edu

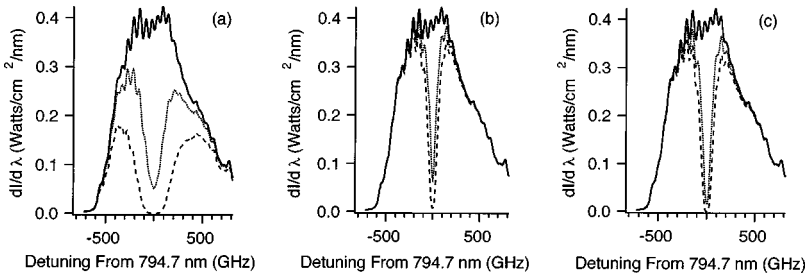

FIG. 1. A typical profile of intensity vs. wavelength for the $GaAl_xAs_{1-x}$ laser diode arrays (Optopower part number OPC-A015-795-FCPS) used in our lab, indicated by a solid line. The total power output per laser is about 15 W. The dotted and dashed lines show the laser profile 5 and 10 cm into the cell, respectively, for cell parameters of: (a) 10 amagat of ^{3}He and 0.1 amagat N_2 at 180 °C (left); (b) 0.1 amagat of ^{129}Xe, 0.2 amagat N_2, and 2.7 amagat He at 110 °C (center); and (c) 2.2 amagat of ^{129}Xe, 0.2 amagat N_2, and 0.5 amagat He at 110 °C (right).

for ^{3}He polarization ($[Rb]=10^{14-15}/cm^3$) is the main reason polarization with LDAs can be so effective for ^{3}He.

The situation is quite different for ^{129}Xe. The spin destruction rate of Rb due to ^{129}Xe is so much greater than that due to ^{3}He that a much greater laser intensity or spectral density (or both) is required to satisfy $\gamma_{opt} \gg \Gamma_{SD}$. Consequently, only a much narrower part of the LDA spectrum is useful for ^{129}Xe, even at very low xenon concentration, as illustrated in Figs. 1(b) and 1(c). Driehuys *et al.* have shown that at high laser intensity (e.g., 50 W/5 cm^2) broadening the Rb absorption line with a buffer gas that does not appreciably increase Γ_{SD}, such as helium, significantly improves Rb polarization.[5] Practical considerations may limit buffer gas pressure, and high laser powers may introduce heating problems (especially in the case of spin–exchange pumped masers), motivating alternative approaches.

The problem of balancing tradeoffs of noble gas polarization, production rates, volumes, and magnetization involves exploring a large parameter space. For example, increasing the total density of gas produces pressure broadening of the Rb absorption line, increases the integral γ_{opt}, but may also appreciably increase Γ_{SD}. Greater Rb density increases γ_{SE} but also increases Γ_{SD} and the attenuation of the light as it propagates through the pumping cell, reducing γ_{opt} further into the cell. Calculations based on the framework presented in Ref. 7 allow us to explore the tradeoffs with a given goal for a given application.

Optical pumping simulations are based on numerical integration of laser light attenuation given by

$$\frac{d\Phi(\mathbf{r},\nu)}{dz} = -\sigma(\nu)[A]\Phi(\mathbf{r},\nu)[1-P_A(\mathbf{r})]. \quad (6)$$

The Rb polarization at any position in the cell can be found as long as the incident intensity and spectral profile are known. We have found that our simulations generally predict results for ^{129}Xe polarization that are within 5%–10% of measured polarizations.[6]

Significant improvement of ^{129}Xe polarization is possible if the LDA light is spectrally narrowed. In Fig. 2, we show a calculation of the expected ^{129}Xe polarizations for different combinations of xenon density, temperature (i.e., Rb density), and laser FWHM for 15 W of laser power. The total pressure is held constant at 2.8 amagat; for example, with 1.0 amagat xenon, we use 0.l amagat N_2, and 1.7 amagat helium. We show results for four gas mixtures, two of which are: (1) a low xenon density of 0.13 amagat xenon and high helium buffer gas density, and (2) a high xenon density of 2.0 amagat xenon described by Rosen *et al.*[6] Narrowing an LDA spectrum provides significant gains in all cases.

Several authors have reported work on narrowing 500 mW LDAs. Single spectral mode output has been achieved with grating feedback,[18,19] but the output powers reported are at least an order of magnitude below that which would be useful for current applications (e.g., medical imaging applications). A grating combined with a photorefractive phase-conjugate mirror has been used to narrow LDAs and LDA bars with more than 50% of the free-running LDA power coupled into less than 0.03 nm bandwidth.[20] Our approach to narrowing LDAs is based on the standard external-cavity laser used widely in atomic physics.[21] We used the Littman–Metcalf configuration as shown in Fig. 3 with a 2 W InGaAsP laser diode array from Coherent Semiconductor Group.[22] These are off-the-shelf lasers mounted in the ''C block'' and were not antireflection (AR) coated or specially prepared in any other way. The temperature of the C block was controlled by standard techniques. The laser output was collimated with standard optics, and the grating was oriented such that the plane of reflection contains the laser's narrow (2 μm) dimension, along which the light is nearly single mode and can be well collimated. To improve the finesse, the beam from the laser hit the 2400 line/mm grating at grazing incidence, increasing the total number of grating lines interacting with the free-running laser. The output beam was the zeroth-order, specular reflection from the grating, which contained 67% of the power incident on the grating from the LDA. The optics and cavity were set up such that an image of the facet was reflected back on the facet by the first order reflection. Spectra were obtained by an optical spectrum analyzer with a fixed grating and a linear charge coupled device (CCD) array. This setup was calibrated using the Rb hyper-

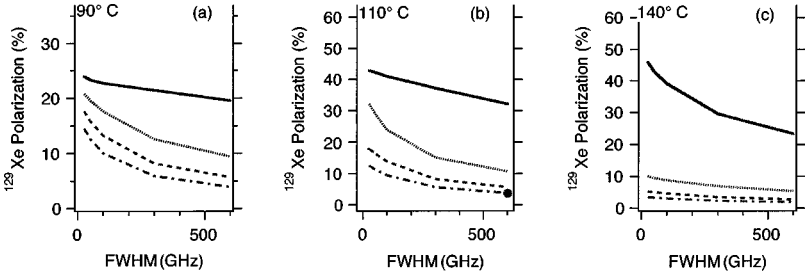

FIG. 2. Calculated ^{129}Xe polarization as a function of the laser diode array line width (full width at half maximum) for 15 W of laser power. For each temperature, curves for 0.13 amagat, 0.65 amagat, 1.3 amagat, and 2 amagat of ^{129}Xe are shown from top to bottom, respectively. A constant total density of 2.8 amagat is maintained by loading with helium buffer gas. The solid dot on (b) the 110° plot (center) shows the measured ^{129}Xe polarization for the 2 amagat ^{129}Xe curve.

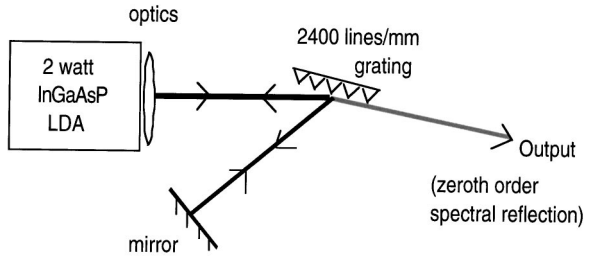

FIG. 3. Littman–Metcalf configuration used to narrow the 2 W laser diode array. The laser hit the 2400 lines/mm holographic grating at grazing incidence, increasing the total number of grating lines interacting with the free-running laser. The output beam was the zeroth-order, specular reflection from the grating. The optics and cavity were set up such that an image of the facet was reflected back on the facet by the first order reflection.

fine lines. Each CCD pixel spanned 15 GHz. All power levels and spectra reported here correspond to the zeroth-order light reflected from the grating.

Once the cavity was set up at lower power (about 0.2 W), the LDA injection current was increased. Above 1.2 W, the external-cavity and free-running laser modes begin to compete strongly, making it more difficult to find conditions that produce stable spectra. Nevertheless, stable operating conditions could still be found. We believe that this general technique could be used for even higher free-running powers than those reported here.

In Fig. 4, we show spectra for both the free-running and external-cavity configurations for two different power levels. For 1.24 W, the FWHM was 34.6 GHz. For 1.0 W, the FWHM was 20.3 GHz. FWHM values were extracted from a lorentzian fit to the central part of the spectrum. In the external-cavity configuration, the central frequency could be tuned over $\approx 4-6$ nm. The setup is quite robust, staying locked indefinitely.

We have used the measured profiles for both configurations to calculate expected performance for a range of xenon densities as described above. Using the measured 1.24 W profile we find that the single 15 W LDA shown in Fig. 1 could be replaced by 3 W of external-cavity LDA light. For the spin exchange pumped maser,[2] heating effects from the high powered LDAs are a problem and we expect significant advantages using an external-cavity LDA. With the commercial availability of 4 W broad area LDAs, 3 W may be possible with a single device.

Competition between the free-running laser and external-cavity laser may be reduced by AR coating the LDA. This would suppress the free-running laser and may allow for higher powered, more stable, frequency-narrowed operation. For the work cited above, an Al-coated, holographic grating was used. A grating with a higher reflectivity, such as a properly blazed, gold-coated, ruled grating, would allow the zeroth order specular reflection power to increase. The 2 W array we used is similar to a single facet of a typical multiarray bar. For most commercially available continuous wave LDA bars, the filling factor is only 30%, making efficient optical feedback from the grating difficult. However, LDA bars that are intended for pulsed use are available with filling factors up to 90%. Thermal management problems limit the duty factor of these in normal operation, but reliable operation might be feasible for 10 W or more.

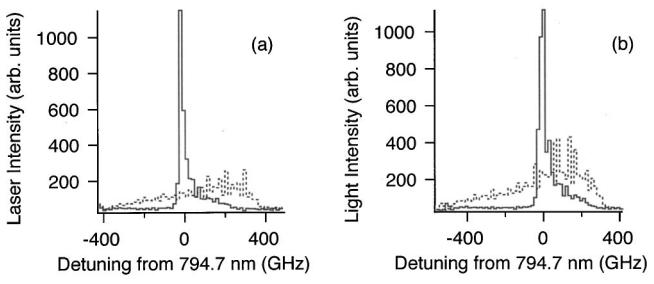

FIG. 4. Frequency profiles of the free-running laser (dotted line) and the grating-narrowed case (solid line). (a) shows 1.0 W with FWHM=20.3 GHz and (b) shows 1.24 W with FWHM=34.6 GHz.

In conclusion, narrowing the spectral profile of high powered LDAs and LDA bars is highly desirable for polarization of ^{129}Xe that is used in medical imaging and other applications. Improvement by factors of nearly 10, or perhaps more, in power requirements or polarization rates can be expected with narrowed arrays. External-cavity laser configurations have been successfully used to narrow the 2 nm output to less than 0.1 nm FWHM.

While preparing this letter, the authors became aware of the work of Thad Walker and his collaborators at the University of Wisconsin, who have also studied narrowing of LDAs in external-cavity configurations and measured ^{129}Xe polarization rates. The authors gratefully acknowledge useful discussion with Leo Hollberg, Georg Raithel, Matt Rosen, and Ralph Conti. This work was partially funded by the NSF and would not have been possible without the lasers provided by the Coherent Semiconductor Group.

[1] T. E. Chupp, R. A. Loveman, A. K. Thompson, A. M. Bernstein, and D. R. Tieger, Phys. Rev. C **45**, 915 (1992).
[2] T. Chupp, R. Hoare, R. Walsworth, and B. Wu, Phys. Rev. Lett. **72**, 2363 (1994).
[3] R. Stoner, M. Rosenberry, J. Wright, T. Chupp, E. Oteiza, and R. Walsworth, Phys. Rev. Lett. **77**, 3971 (1996).
[4] M. Albert, G. Cates, B. Driehuys, W. Happer, C. Springer, B. Saam, and A. Wishnia, Nature (London) **370**, 199 (1994).
[5] B. Driehuys, G. Cates, E. Miron, K. Sauer, D. Walker, and W. Happer, Appl. Phys. Lett. **69**, 1668 (1996).
[6] M. S. Rosen, T. E. Chupp, K. P. Coulter, R. C. Welsh, and S. D. Swanson, Rev. Sci. Instrum. **70**, 1546 (1999).
[7] M. Wagshul and T. Chupp, Phys. Rev. A **24**, 827 (1989).
[8] W. Kastler, J. Phys. Radium **11**, 225 (1950).
[9] W. Happer, Rev. Mod. Phys. **44**, 169 (1972).
[10] M. A. Bouchiat, and T. C. and C. M. Varnum, Phys. Rev. Lett. **5**, 373 (1960).
[11] M. Aymar, M. Bouchiat, and J. Brossel, Phys. Lett. **24A**, 753 (1967).
[12] W. Happer, E. Miron, S. Schaefer, D. Schreiber, W. van Wijngaarden, and X. Zeng, Phys. Rev. A **29**, 3092 (1984).
[13] X. Zeng, Z. Wu, T. Call, E. Miron, D. Schreiber, and W. Happer, Phys. Rev. A **31**, 260 (1985).
[14] T. E. Chupp, M. E. Wagshul, K. Coulter, A. B. McDonald, and W. Happer, Phys. Rev. C **36**, 2244 (1987).
[15] M. Wagshul and T. Chupp, Phys. Rev. A **49**, 3854 (1994).
[16] T. Walker and W. Happer, Rev. Mod. Phys. **69**, 629 (1997).
[17] S. Appelt, A. B.-A. Baranga, C. Erickson, M. Romalis, A. Young, and W. Happer, Phys. Rev. A **58**, 1412 (1998).
[18] A. F. den Boer, K. A. H. van Leeuween, H. C. W. Beijerinck, C. Fort, and F. Pavone, Appl. Phys. B: Lasers Opt. **63**, 117 (1996).
[19] M. Løbel, P. M. Petersen, and P. M. Johansen, Opt. Lett. **23**, 825 (1998).
[20] M. Løbel, P. M. Petersen, and P. M. Johansen, J. Opt. Soc. Am. B **15**, 2000 (1998).
[21] K. B. MacAdam, A. Steinbach, and C. Wieman, Am. J. Phys. **60**, 1098 (1992).
[22] Coherent Semiconductor Group, PartNumber S-709-2000C-150-C.